

Measurement of the Polarized Forward-Backward Asymmetry of $Z^0 \rightarrow b\bar{b}$ Using a Lifetime Tag and Momentum-Weighted Track Charge

The SLD Collaboration ¹

*Stanford Linear Accelerator Center
Stanford University
Stanford, CA 94309*

ABSTRACT

We present a direct measurement of the parity-violating parameter A_b by analyzing the left-right forward-backward asymmetry of b quarks in $e^+e^- \rightarrow Z^0 \rightarrow b\bar{b}$. The SLD experiment observes hadronic decays of Z^0 bosons produced at resonance in collisions of longitudinally polarized electrons and unpolarized positrons at the SLC. Heavy flavor decays of the Z^0 are identified by taking advantage of the long lifetime of B hadrons, the small, stable SLC beam spot, and precise tracking from SLD. The asymmetry A_b is measured with a self-calibrating technique employing momentum-weighted track charge from both hemispheres in the tagged events. From our 1994-1995 sample of 3.6 pb^{-1} of e^+e^- annihilation data with a luminosity-weighted average e^- polarization of 77.3%, and our 1993 sample of 1.8 pb^{-1} with a luminosity-weighted polarization of 63.1%, we obtain $A_b(\text{preliminary}) = 0.843 \pm 0.046(\text{stat.}) \pm 0.051(\text{syst.})$.

Submitted to the 1995 International Europhysics Conference on High Energy Physics (HEP95)

¹Work supported by U.S. Department of Energy contract #DE-AC03-76SF00515.

1 Introduction

Measurements of fermion production asymmetries at the Z^0 pole provide probes of the combination of vector (v) and axial vector (a) couplings $A_f = 2v_f a_f / (v_f^2 + a_f^2)$, which express the extent of parity violation in the Zff coupling. At Born level, the Z^0 peak differential cross section for producing a final state fermion f at an angle $z = \cos \theta$ from the electron beam direction is

$$\sigma^f(z) \equiv d\sigma_f/dz \propto (1 - A_e P_e)(1 + z^2) + 2A_f(A_e - P_e)z, \quad (1)$$

where P_e is the longitudinal polarization of the electron beam. By manipulating the sign of P_e , it is possible to measure the left-right forward-backward asymmetry for b quark production [1]

$$\tilde{A}_{FB}^b(z) = \frac{[\sigma_L^b(z) - \sigma_L^b(-z)] - [\sigma_R^b(z) - \sigma_R^b(-z)]}{\sigma_L^b(z) + \sigma_L^b(-z) + \sigma_R^b(z) + \sigma_R^b(-z)} = |P_e| A_b \frac{2z}{1 + z^2}, \quad (2)$$

where L, R refers to $Z^0 \rightarrow b\bar{b}$ decays produced with a predominantly left-handed (negative helicity) or right-handed (positive helicity) electron beam, respectively. The measurement of the double asymmetry eliminates the dependence on the Zee coupling parameter A_e . The quantity A_b is largely independent of propagator effects that modify the effective weak mixing angle ($\delta A_b = -0.63 \cdot \delta \sin^2 \theta_W^{eff}$), and thus is complementary to other electroweak asymmetry measurements performed at the Z^0 pole.

In this paper we present an updated measurement of $\tilde{A}_{FB}^b(z)$ using an impact parameter tag to select an enriched sample of $Z^0 \rightarrow b\bar{b}$ events, and the net momentum-weighted track charge, first suggest by Feynman and Field [2], to identify the sign of the charge of the underlying b quark. This technique was pioneered at lower energies [3], and most recently applied at the Z^0 in conjunction with a lifetime tag [4][5][6]. The first direct measurements of the extent of parity violation in the Zbb coupling were made by SLD using momentum-weighted track charge [7] and leptons from semileptonic B hadron decay [8]. The analysis presented in this paper is based on momentum-weighted track charge with an improved calibration technique which greatly reduces model dependence.

The operation of the SLAC Linear Collider (SLC) with a polarized electron beam has been described previously [9]. During the 1993 running period, the SLD Large Detector (SLD) recorded 1.8 pb^{-1} of e^+e^- annihilation data at a mean center-of-mass energy of $91.26 \pm 0.02 \text{ GeV}$, with a mean electron beam longitudinal polarization of $(63 \pm 1)\%$. In 1994–1995, SLD recorded 3.6 pb^{-1} at the same energy, but with a mean longitudinal polarization of $(77 \pm 1)\%$. Charged particles were tracked in the Central Drift Chamber (CDC) [10] in a uniform axial magnetic field of 0.6 T . In addition, a pixel-based silicon vertex detector (VXD) [11] provides an accurate measure of particle trajectories close to the beam axis. The momentum resolution of the combined CDC and VXD systems is $(\delta p_\perp / p_\perp)^2 = (.01)^2 + (.0026 p_\perp)^2$, where p_\perp is the momentum in GeV/c perpendicular to the beamline. The thrust axis [12] was reconstructed using the Liquid Argon Calorimeter [13], which covers a range of $|\cos \theta| < 0.98$.

2 Lifetime Tag and Momentum-Weighted Track Charge

The accurate impact parameter measurement provided by the addition of the VXD information to the CDC tracks was used to select a sample enriched in $Z^0 \rightarrow b\bar{b}$ events. The impact parameter d was derived by applying a sign to the distance of closest approach such that d is positive when the vector from the IP to the point at which the track intersects the associated jet axis [15] makes an acute angle with respect to the track direction. All impact parameters used in this analysis were for tracks projected into the plane perpendicular to the beam axis, and were measured with respect to the SLC interaction point (IP), derived from fits to Z^0 decays close in time to the event under study [9]. Including the uncertainty on the average IP position, the impact parameter uncertainty σ_d for the overall tracking system approaches $13 \mu m$ for high momentum tracks, and is $76 \mu m$ at $p_{\perp} \sqrt{\sin \theta} = 1 \text{ GeV}/c$.

For the purpose of selecting hadronic events and calculating the momentum-weighted track charge, a loose set of requirements was placed on reconstructed tracks, while stricter requirements were placed on tracks used to select $Z^0 \rightarrow b\bar{b}$ candidates. “Track-charge quality” tracks were required to have: i) $p_{\perp} \geq 0.15 \text{ GeV}/c$ and $p_{tot} < 50 \text{ GeV}/c$; ii) $|\cos \theta| \leq 0.8$; and iii) point of closest approach to the beam line within a cylinder of radius r_0 and half-length l_0 about the IP of $(r_0, l_0) = (2.0, 10.0) \text{ cm}$. “Impact parameter quality” tracks were additionally required to have: i) the point of closest approach within $(r_0, l_0) = (0.3, 1.5) \text{ cm}$; ii) at least one VXD hit; iii) $\sigma_d < 250 \mu m$; and iv) not been identified as a decay product of a Λ , K_s^0 , or γ -conversion.

Events were classified as hadronic decays of the Z^0 provided that they contained at least 7 track-charge quality tracks, a visible charged energy of at least 20 GeV, and a thrust axis satisfying $|\cos \theta_{thrust}| < 0.7$. The resulting hadronic sample contained 15,858 events (1993, omitting data in a period with a biased trigger) and 59430 events (1994–1995), with $< 0.1\%$ non-hadronic background.

A $Z^0 \rightarrow b\bar{b}$ enriched sample of 2504 events (1993) and 9498 events (1994–1995) was identified by selecting hadronic events with three or more impact parameter quality tracks with normalized impact parameter $d/\sigma_d > 3.0$ [14]. Monte Carlo (MC) studies indicate that this selection is 61% efficient for identifying $Z^0 \rightarrow b\bar{b}$ events, with a purity of 89%.

Using all track-charge quality tracks, we formed the event momentum-weighted charge sum [2]

$$Q = - \sum_{tracks} q_i \cdot \text{sgn}(\vec{p}_i \cdot \hat{T}) |(\vec{p}_i \cdot \hat{T})|^{\kappa}, \quad (3)$$

as well as the hemisphere summed momentum-weighted charge

$$Q_s = \sum_{tracks} q_i |(\vec{p}_i \cdot \hat{T})|^{\kappa}, \quad (4)$$

where q_i and \vec{p}_i are the track charge and momentum, and \hat{T} is the unit vector in the direction of the reconstructed thrust axis, signed so that $Q > 0$, making \hat{T} an

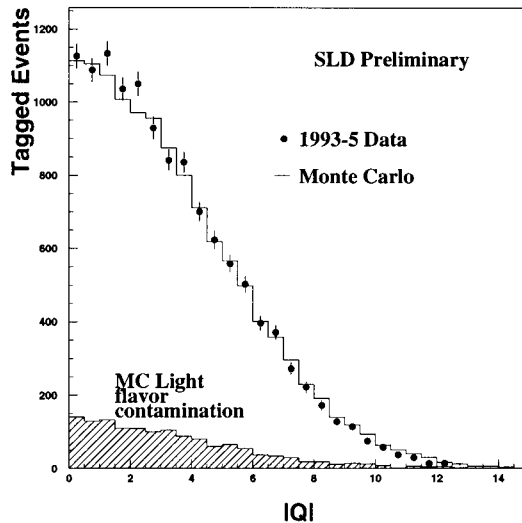


Figure 1: Comparison of the momentum-weighted charge $|Q|$ between data and Monte Carlo

estimate of the b quark direction. We have chosen $\kappa = 0.5$ to maximize the analyzing power (AP) of the track charge algorithm for $Z^0 \rightarrow b\bar{b}$ events

$$AP = \frac{P_{cor} - P_{inc}}{P_{cor} + P_{inc}} \simeq 37\%, \quad (5)$$

where P_{cor} (P_{inc}) is the probability of assigning the b quark to the correct (incorrect) thrust hemisphere. Figure 1 shows a comparison of the Q distribution between data and MC. Figure 2 shows the \hat{T}_z distribution for the enriched sample separately for left- and right-handed electron beam.

3 Maximum-Likelihood Analysis

The technique used to extract A_b from the data is a self-calibrated Maximum-Likelihood analysis, which takes advantage of the fact that the two hemispheres of a tagged event provide separate momentum-weighted track charges, which provide nearly independent information about the direction of the b quark. The likelihood function chosen for this analysis is based on the differential cross-section of Equation 1:

$$\ln \mathcal{L} = \sum_{events} \ln(p(event_i, A_b, A_c)), \quad (6)$$

with

$$p(event_i, A_b, A_c) = (1 - A_e P_e^i)(1 + \cos^2 \theta_i) + 2(A_e - P_e^i) \cos \theta_i [\\ A_b f_i^b (2p_i^{correct,b} - 1)(1 - \Delta_{QCD,b}^i) + \\ A_c f_i^c (2p_i^{correct,c} - 1)(1 - \Delta_{QCD,c}^i) + \\ A_{bckg} (1 - f_i^b - f_i^c) (2p_i^{correct,bckg} - 1)], \quad (7)$$

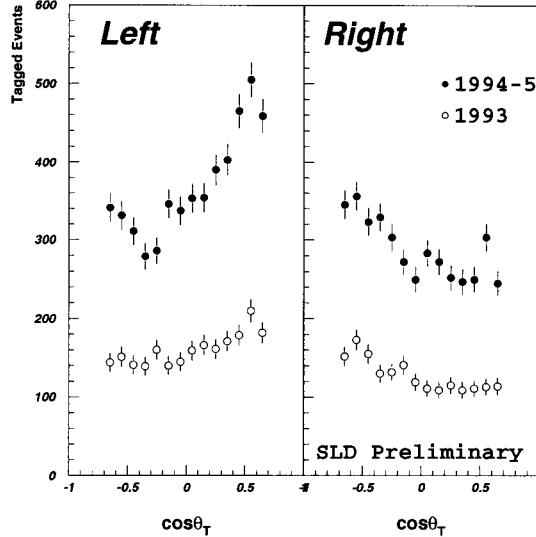


Figure 2: Distribution of the signed thrust axis in the 1993-1995 tagged sample. A clear forward-backward asymmetry is observed, with sign as expected from the cross section formula in Equation 1.

where A_e is the asymmetry in electron coupling to the Z^0 , P_e^i is the signed polarization of the electron beam when that event was recorded, $f_i^{b(c)}$ are the probabilities that that event was a $Z^0 \rightarrow b\bar{b}(c\bar{c})$ decay, and are parameterized as a function of the number of tracks missing the origin by 3σ , and $\Delta_{QCD,b,c}^i$ are final-state QCD corrections, to be discussed in Sections 3.3 and 4. A_{bckg} is an estimated asymmetry from $u\bar{u}$, $d\bar{d}$, and $s\bar{s}$ decays of the Z^0 . The correct-sign probabilities $p^{correct,b}$ and $p^{correct,c}$ are estimated as functions of the momentum weighted charge $|Q|$, defined in Equation 3. The $p^{correct,b,c}(|Q|)$ parameterize how well the algorithm signs the thrust axis and may be estimated from the Monte Carlo, but $p^{correct,b}$ can be inferred from the data with a much reduced model dependence.

While A_e appears in the likelihood function of Equation 7, the dependence of the fit A_b on the assumed value of A_e is very small and must vanish in the limit of large statistics. This can be seen by dividing Equation 7 by $(1 - A_e P_e^i)$, which does not affect the fit. If the data is then analyzed with $P_e^i = \pm 1$, retaining only the sign of the polarization on each event, then the likelihood function would be manifestly independent of A_e . The value of A_b would then be extracted by dividing the resulting fit value by the luminosity-weighted average polarization $\langle P_e \rangle_{\mathcal{L}}$. The only differences in the fit results arising from using an event-by-event polarization or dividing by a luminosity-weighted polarization after the fit are statistical in nature.

3.1 Calibrating the Analyzing Power

The functional form of $p^{correct,b}(|Q|)$ can be derived with the aid of two assumptions about the hemisphere momentum-weighted charge distributions. These assumptions are that the momentum-weighted charge in the b hemisphere, Q_b , and the momentum-weighted charge in the \bar{b} hemisphere, $Q_{\bar{b}}$, are Gaussian and uncorrelated. The effect of interhemisphere correlation will be incorporated in Section 3.2. There is also an assumption that the decays preserve CP symmetry, in that $\langle Q_b \rangle$ is assumed to be $-\langle Q_{\bar{b}} \rangle$, and that the widths of the two distributions are the same. The most significant violation of CP in this analysis arises from interactions with the detector material, which add excess positive charge to both hemispheres. This effect will be discussed in Section 4.

With these assumptions, a calibration procedure for the correct-sign probability using the momentum-weighted charges in the two hemispheres may be formulated. The quantities

$$Q_{sum} = Q_b + Q_{\bar{b}} \quad (8)$$

and

$$Q_{diff} = Q_b - Q_{\bar{b}} \quad (9)$$

are identifiable with observable variables: $Q_{sum} = Q_s$, and $|Q_{diff}| = |Q|$, defined in Equations 4 and 3. The correct-sign probability $p^{correct,b}(|Q|)$ is the fraction the time $Q_{diff} < 0$ when $|Q_{diff}| = |Q|$. The task is to find the mean q_0 and width σ of the Gaussian Q_{diff} distribution. With these in hand,

$$p^{correct,b}(|Q|) = \frac{1}{1 + e^{-\alpha_b |Q|}}, \quad (10)$$

with

$$\alpha_b = 2q_0/\sigma^2. \quad (11)$$

These two variables can be easily obtained from the data:

$$\sigma = \sigma_{sum} = \sqrt{\langle Q_s^2 \rangle}, \quad (12)$$

and

$$q_0 \simeq \sqrt{2(\sigma_{sum}\sigma_{diff} - \sigma_{sum}^2)}, \quad (13)$$

where

$$\sigma_{diff} = \sqrt{\langle Q_{diff}^2 \rangle} = \sqrt{\langle Q^2 \rangle} \quad (14)$$

is the width of a single Gaussian with zero mean fitted to the $|Q|$ distribution.

3.2 Interhemisphere Correlation

While this calibration of the correct-sign probability accounts for nearly all of the charge-diluting effects present in the data, a departure from the uncorrelated probability assumption produces a shift in the α_b derived in the last section. This correlation arises because of the nature of the hadronization process, which demands total charge

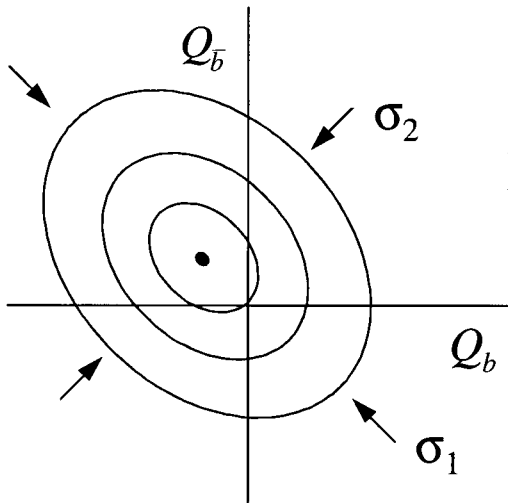


Figure 3: Effect of inter-hemisphere correlations on the momentum-weighted charge distributions.

conservation in the event, and tracks which migrate from one thrust hemisphere to the other.

The effect of correlation is to distort the joint probability of Q_b and $Q_{\bar{b}}$ from a circular Gaussian distribution to a Gaussian ellipsoid, stretched along one of the 45° diagonals, shown in Figure 3. The effect is to change σ_1 , the width of the signed Q_{diff} distribution, relative to σ_2 , the width of the signed Q_{sum} distribution:

$$\sigma_1 = (1 + \lambda)\sigma_2. \quad (15)$$

The uncorrelated hypothesis used the same value for these two, σ_{sum} . The correlation is incorporated into the analysis by using $(1 + \lambda)\sigma_{sum}$ in the expression for α_b :

$$\alpha = \frac{2\sqrt{2\left(\frac{\sigma_{diff}}{(1+\lambda)\sigma_{sum}} - 1\right)}}{(1 + \lambda)\sigma_{sum}}. \quad (16)$$

The correlation λ has been estimated to be 2.9% using JETSET 7.4 [18] with parton shower evolution and string fragmentation, and full detector simulation.

3.3 Measurement of A_b

To determine α_b , the data σ_{sum} and σ_{diff} are corrected for light-flavor contamination in the tag, which modifies α_b by a small amount. The value of α_b is also allowed to vary as a function of $\cos\theta$, owing to the geometrical tracking acceptance, and so a Monte Carlo model of its dependence on polar angle is scaled to the overall α_b measured from tagged events in the data.

The remaining ingredients to the likelihood function of Equation 7 are obtained from Monte Carlo: the bottom and charm probabilities f^b and f^c , and $p^{correct,c}$. The

Table 1: Calibration parameters for the data and Monte Carlo. Errors are statistical only.

	Data	Monte Carlo
σ_{sum}	3.669 ± 0.023	3.791 ± 0.010
σ_{diff}	4.205 ± 0.027	4.345 ± 0.011
λ	assume same as MC	0.029
α_b	0.253 ± 0.013	0.245 ± 0.005

value of A_c is set to its Standard Model value of 0.67, and the value of A_{bckg} is set to zero. The error arising from the latter is very small owing to its $\sim 1\%$ fraction in the tagged sample.

It has been noted that the hemisphere calibration technique accounts for a portion of the QCD radiative correction [5]. Events with both the quark and antiquark in the same hemisphere do not sign properly as often as the remainder of the sample, and this effect is taken into account by the calibration procedure. Angular smearing of the thrust axis in events with hard gluon radiation accounts for the remainder of the QCD correction.

The values of $\Delta_{QCD}^{b,c}(\cos\theta)$ incorporated in this analysis are $\cos\theta$ -dependent calculations first-order in α_s , including the mass of the B quark [19]. Because this analysis makes use of the thrust axis, which is a slightly more reliable estimate of the decay axis than either quark's jet axis, the value of the QCD correction is estimated [17] to be slightly less ($\sim 90\%$) of the correction calculated assuming the b axis is measured.

The value of A_b fit with the likelihood function is $A_b = 0.843 \pm 0.046$ (*stat*).

4 Systematic Errors

Systematic errors arise from the use of Monte Carlo modeling in the likelihood fit, and the statistical power of the fit for α_b . The statistical error on σ_{sum} and σ_{diff} in the data will scale with $1/\sqrt{N}$. The validity of the Gaussian assumption for the shape of Q_b and $Q_{\bar{b}}$ was checked with a simulation that generated various triangular distributions as well as a double Gaussian with tails, and only small deviations were seen in the fit A_b when the underlying shape was modified. The shape of Q_{sum} in the data constrains the shape of $p(Q_b)$ to be Gaussian. Because $|Q_b|$ and $|Q_{\bar{b}}|$ share the same probability distribution, that distribution is observable in the data and may also be used to provide tighter constraints on the Gaussian shape hypothesis. No deviations from the Gaussian hypothesis were seen, and the trial functions were ruled out with high confidence.

Different models were chosen for the $\cos\theta$ dependence of the α_b shape, but since the overall scale is determined by that in the data, the effect on the measured

A_b is small.

One of the largest errors in the analysis involves the estimation of the inter-hemisphere correlation. At this point, our conservative approach is to compare the correlations estimated using the JETSET 7.4 generator with string fragmentation, the JETSET generator with independent fragmentation, and the HERWIG 5.7 generator. Varying the detector's angular acceptance in the simulation was found to have a negligible effect on the correlation.

The correlation estimated with the JETSET's string fragmentation model is relatively insensitive to model parameters expected to affect it. Variations in the diquark popping parameter (PARJ(1)=0.20, default: 0.10), the energy cutoff for fragmentation stopping (PARJ(33)=1.50, default: 0.80), the dependence on the mass of the final quark on the stopping energy (PARJ(36)=1.0, default: 2.0), the endpoint energy smearing (PARJ(37)=1.0, default: 0.2), the reverse rapidity ordering probability for the last two hadrons popped (PARJ(38)=1.0, default: 2.5), and the vector fraction for light mesons (PARJ(11)=0.6, default: 0.5), were made. Variations in the resulting estimates of the correlation were less than 7% of the correlation value. The HERWIG 5.7 generator, on the other hand, estimates a correlation $\sim 27\%$ larger than JETSET's, and the independent fragmentation model has a correlation $\sim 31\%$ smaller than the string model. We take the difference between the independent fragmentation model's correlation and the string fragmentation model's as an estimate of the systematic error.

The models of the sum and difference widths of the tagged u , d , s , and c events are close to the observed b sum and difference widths, so the correction to α_b from their presence in the tag is minimal. Another source of error investigated is the effect of nuclear scattering of final-state hadrons with the material of the detector. The effect is to broaden the distributions of both Q_b and $Q_{\bar{b}}$, and to bias both by adding a small average positive charge. The increased width dilutes the charge identification in a way that is calibrated by the technique. The positive bias introduces an extra width which must be subtracted in quadrature from σ_{sum} . This extra average charge may be measured in the data by calculating $\langle Q_{sum} \rangle$, and is estimated to be 0.05/hemisphere for $\kappa = 0.5$. Because $\sigma_{sum} = 3.79$, this effect is negligible.

The dominant model errors come from estimations of the tag purity and the value of A_c assumed. Most of the uncertainties in the modeling of the tag affect the efficiency of tagging $Z^0 \rightarrow b\bar{b}$, and thus have only a secondary effect on the purity of the tag. The leading uncertainties in the purity of the tag arise from the available knowledge of R_c and from the decay multiplicity of charmed hadrons[14]. This error may decrease with a larger data sample by the introduction of a double tag; only R_b need be assumed, and it is measured with high precision.

The error on the QCD correction is conservatively estimated at twice the value of the uncertainty in the experimental determination of $\alpha_s(M_Z)$ arising from theoretical ambiguity, summed in quadrature with the full value of the second-order contribution calculated in [16].

The combined 1993-1995 SLD measurement of A_b using momentum-weighted

Table 2: Relative systematic errors on the measurement of A_b .

Error Source	Variation	$\delta A_b/A_b$
<i>Self-Calibration</i>		
α_b statistics	1σ	3.4%
$P(Q_b)$ shape	Triangular, other shapes	1.0%
$\cos\theta$ dependence of α_b	other shapes	1.5%
Hemisphere Correlation	Independent Frag.	3.7%
Light Flavor Subtraction	100% of correction	0.2%
Detector Material	100% of correction	0.1%
<i>Analysis</i>		
A_c	0.67 ± 0.07	1.0%
A_{bckg}	0 ± 0.50	0.6%
A_e	0.15 ± 0.02	0.1%
α_c	mostly $x_D \pm 5\%$	0.2%
Tag Composition	Mostly $R_c = 0.171 \pm 0.017$	2.6%
Beam Polarization	-	0.8%
QCD	2^{nd} order terms and $\alpha_s \pm 0.2$	0.9%
Total		6.2%

track charge is

$$A_b(\text{Preliminary}) = 0.843 \pm 0.046(\text{stat.}) \pm 0.051(\text{syst.}), \quad (17)$$

consistent with the Standard Model prediction of 0.94.

5 Acknowledgments

We thank the personnel of the SLAC accelerator department and the technical staffs of our collaborating institutions for their outstanding efforts on our behalf. We also thank H. Olsen and J. Stav for helpful discussions relating to this analysis.

The SLD Collaboration

K. Abe,⁽²⁹⁾ I. Abt,⁽¹⁴⁾ C.J. Ahn,⁽²⁶⁾ T. Akagi,⁽²⁷⁾ N.J. Allen,⁽⁴⁾ W.W. Ash,^{(27)†}
 D. Aston,⁽²⁷⁾ K.G. Baird,⁽²⁵⁾ C. Baltay,⁽³³⁾ H.R. Band,⁽³²⁾ M.B. Barakat,⁽³³⁾
 G. Baranko,⁽¹⁰⁾ O. Bardon,⁽¹⁶⁾ T. Barklow,⁽²⁷⁾ A.O. Bazarko,⁽¹¹⁾ R. Ben-David,⁽³³⁾
 A.C. Benvenuti,⁽²⁾ T. Bienz,⁽²⁷⁾ G.M. Bilei,⁽²²⁾ D. Bisello,⁽²¹⁾ G. Blaylock,⁽⁷⁾
 J.R. Bogart,⁽²⁷⁾ T. Bolton,⁽¹¹⁾ G.R. Bower,⁽²⁷⁾ J.E. Brau,⁽²⁰⁾ M. Breidenbach,⁽²⁷⁾
 W.M. Bugg,⁽²⁸⁾ D. Burke,⁽²⁷⁾ T.H. Burnett,⁽³¹⁾ P.N. Burrows,⁽¹⁶⁾ W. Busza,⁽¹⁶⁾
 A. Calcaterra,⁽¹³⁾ D.O. Caldwell,⁽⁶⁾ D. Calloway,⁽²⁷⁾ B. Camanzi,⁽¹²⁾
 M. Carpinelli,⁽²³⁾ R. Cassell,⁽²⁷⁾ R. Castaldi,^{(23)(a)} A. Castro,⁽²¹⁾ M. Cavalli-Sforza,⁽⁷⁾
 E. Church,⁽³¹⁾ H.O. Cohn,⁽²⁸⁾ J.A. Coller,⁽³⁾ V. Cook,⁽³¹⁾ R. Cotton,⁽⁴⁾
 R.F. Cowan,⁽¹⁶⁾ D.G. Coyne,⁽⁷⁾ A. D'Oliveira,⁽⁸⁾ C.J.S. Damerell,⁽²⁴⁾ M. Daoudi,⁽²⁷⁾
 R. De Sangro,⁽¹³⁾ P. De Simone,⁽¹³⁾ R. Dell'Orso,⁽²³⁾ M. Dima,⁽⁹⁾ P.Y.C. Du,⁽²⁸⁾
 R. Dubois,⁽²⁷⁾ B.I. Eisenstein,⁽¹⁴⁾ R. Elia,⁽²⁷⁾ E. Etzion,⁽⁴⁾ D. Falciari,⁽²²⁾
 M.J. Fero,⁽¹⁶⁾ R. Frey,⁽²⁰⁾ K. Furuno,⁽²⁰⁾ T. Gillman,⁽²⁴⁾ G. Gladding,⁽¹⁴⁾
 S. Gonzalez,⁽¹⁶⁾ G.D. Hallewell,⁽²⁷⁾ E.L. Hart,⁽²⁸⁾ Y. Hasegawa,⁽²⁹⁾ S. Hedges,⁽⁴⁾
 S.S. Hertzbach,⁽¹⁷⁾ M.D. Hildreth,⁽²⁷⁾ J. Huber,⁽²⁰⁾ M.E. Huffer,⁽²⁷⁾ E.W. Hughes,⁽²⁷⁾
 H. Hwang,⁽²⁰⁾ Y. Iwasaki,⁽²⁹⁾ D.J. Jackson,⁽²⁴⁾ P. Jacques,⁽²⁵⁾ J. Jaros,⁽²⁷⁾
 A.S. Johnson,⁽³⁾ J.R. Johnson,⁽³²⁾ R.A. Johnson,⁽⁸⁾ T. Junk,⁽²⁷⁾ R. Kajikawa,⁽¹⁹⁾
 M. Kalelkar,⁽²⁵⁾ H. J. Kang,⁽²⁶⁾ I. Karliner,⁽¹⁴⁾ H. Kawahara,⁽²⁷⁾ H.W. Kendall,⁽¹⁶⁾
 Y. Kim,⁽²⁶⁾ M.E. King,⁽²⁷⁾ R. King,⁽²⁷⁾ R.R. Kofler,⁽¹⁷⁾ N.M. Krishna,⁽¹⁰⁾
 R.S. Kroeger,⁽¹⁸⁾ J.F. Labs,⁽²⁷⁾ M. Langston,⁽²⁰⁾ A. Lath,⁽¹⁶⁾ J.A. Lauber,⁽¹⁰⁾
 D.W.G. Leith,⁽²⁷⁾ M.X. Liu,⁽³³⁾ X. Liu,⁽⁷⁾ M. Loretì,⁽²¹⁾ A. Lu,⁽⁶⁾ H.L. Lynch,⁽²⁷⁾
 J. Ma,⁽³¹⁾ G. Mancinelli,⁽²²⁾ S. Manly,⁽³³⁾ G. Mantovani,⁽²²⁾ T.W. Markiewicz,⁽²⁷⁾
 T. Maruyama,⁽²⁷⁾ R. Massetti,⁽²²⁾ H. Masuda,⁽²⁷⁾ E. Mazzucato,⁽¹²⁾
 A.K. McKemey,⁽⁴⁾ B.T. Meadows,⁽⁸⁾ R. Messner,⁽²⁷⁾ P.M. Mockett,⁽³¹⁾
 K.C. Moffeit,⁽²⁷⁾ B. Mours,⁽²⁷⁾ G. Müller,⁽²⁷⁾ D. Muller,⁽²⁷⁾ T. Nagamine,⁽²⁷⁾
 U. Nauenberg,⁽¹⁰⁾ H. Neal,⁽²⁷⁾ M. Nussbaum,⁽⁸⁾ Y. Ohnishi,⁽¹⁹⁾ L.S. Osborne,⁽¹⁶⁾
 R.S. Panvini,⁽³⁰⁾ H. Park,⁽²⁰⁾ T.J. Pavel,⁽²⁷⁾ I. Peruzzi,^{(13)(b)} M. Piccolo,⁽¹³⁾
 L. Piemontese,⁽¹²⁾ E. Pieroni,⁽²³⁾ K.T. Pitts,⁽²⁰⁾ R.J. Plano,⁽²⁵⁾ R. Prepost,⁽³²⁾
 C.Y. Prescott,⁽²⁷⁾ G.D. Punkar,⁽²⁷⁾ J. Quigley,⁽¹⁶⁾ B.N. Ratcliff,⁽²⁷⁾ T.W. Reeves,⁽³⁰⁾
 J. Reidy,⁽¹⁸⁾ P.E. Rensing,⁽²⁷⁾ L.S. Rochester,⁽²⁷⁾ J.E. Rothberg,⁽³¹⁾ P.C. Rowson,⁽¹¹⁾
 J.J. Russell,⁽²⁷⁾ O.H. Saxton,⁽²⁷⁾ S.F. Schaffner,⁽²⁷⁾ T. Schalk,⁽⁷⁾ R.H. Schindler,⁽²⁷⁾
 U. Schneekloth,⁽¹⁶⁾ B.A. Schumm,⁽¹⁵⁾ A. Seiden,⁽⁷⁾ S. Sen,⁽³³⁾ V.V. Serbo,⁽³²⁾
 M.H. Shaevitz,⁽¹¹⁾ J.T. Shank,⁽³⁾ G. Shapiro,⁽¹⁵⁾ S.L. Shapiro,⁽²⁷⁾ D.J. Sherden,⁽²⁷⁾
 K.D. Shmakov,⁽²⁸⁾ C. Simopoulos,⁽²⁷⁾ N.B. Sinev,⁽²⁰⁾ S.R. Smith,⁽²⁷⁾ J.A. Snyder,⁽³³⁾
 P. Stamer,⁽²⁵⁾ H. Steiner,⁽¹⁵⁾ R. Steiner,⁽¹⁾ M.G. Strauss,⁽¹⁷⁾ D. Su,⁽²⁷⁾
 F. Suekane,⁽²⁹⁾ A. Sugiyama,⁽¹⁹⁾ S. Suzuki,⁽¹⁹⁾ M. Swartz,⁽²⁷⁾ A. Szumilo,⁽³¹⁾
 T. Takahashi,⁽²⁷⁾ F.E. Taylor,⁽¹⁶⁾ E. Torrence,⁽¹⁶⁾ J.D. Turk,⁽³³⁾ T. Usher,⁽²⁷⁾
 J. Va'vra,⁽²⁷⁾ C. Vannini,⁽²³⁾ E. Vella,⁽²⁷⁾ J.P. Venuti,⁽³⁰⁾ R. Verdier,⁽¹⁶⁾
 P.G. Verdini,⁽²³⁾ S.R. Wagner,⁽²⁷⁾ A.P. Waite,⁽²⁷⁾ S.J. Watts,⁽⁴⁾
 A.W. Weidemann,⁽²⁸⁾ E.R. Weiss,⁽³¹⁾ J.S. Whitaker,⁽³⁾ S.L. White,⁽²⁸⁾
 F.J. Wickens,⁽²⁴⁾ D.A. Williams,⁽⁷⁾ D.C. Williams,⁽¹⁶⁾ S.H. Williams,⁽²⁷⁾
 S. Willocq,⁽³³⁾ R.J. Wilson,⁽⁹⁾ W.J. Wisniewski,⁽⁵⁾ M. Woods,⁽²⁷⁾ G.B. Word,⁽²⁵⁾
 J. Wyss,⁽²¹⁾ R.K. Yamamoto,⁽¹⁶⁾ J.M. Yamartino,⁽¹⁶⁾ X. Yang,⁽²⁰⁾ S.J. Yellin,⁽⁶⁾
 C.C. Young,⁽²⁷⁾ H. Yuta,⁽²⁹⁾ G. Zapalac,⁽³²⁾ R.W. Zdarko,⁽²⁷⁾ C. Zeitlin,⁽²⁰⁾
 Z. Zhang,⁽¹⁶⁾ and J. Zhou,⁽²⁰⁾

- (1) *Adelphi University, Garden City, New York 11530*
 (2) *INFN Sezione di Bologna, I-40126 Bologna, Italy*
 (3) *Boston University, Boston, Massachusetts 02215*
 (4) *Brunel University, Uxbridge, Middlesex UB8 3PH, United Kingdom*
 (5) *California Institute of Technology, Pasadena, California 91125*
 (6) *University of California at Santa Barbara, Santa Barbara, California 93106*
 (7) *University of California at Santa Cruz, Santa Cruz, California 95064*
 (8) *University of Cincinnati, Cincinnati, Ohio 45221*
 (9) *Colorado State University, Fort Collins, Colorado 80523*
 (10) *University of Colorado, Boulder, Colorado 80309*
 (11) *Columbia University, New York, New York 10027*
 (12) *INFN Sezione di Ferrara and Università di Ferrara, I-44100 Ferrara, Italy*
 (13) *INFN Lab. Nazionali di Frascati, I-00044 Frascati, Italy*
 (14) *University of Illinois, Urbana, Illinois 61801*
 (15) *Lawrence Berkeley Laboratory, University of California, Berkeley, California 94720*
 (16) *Massachusetts Institute of Technology, Cambridge, Massachusetts 02139*
 (17) *University of Massachusetts, Amherst, Massachusetts 01003*
 (18) *University of Mississippi, University, Mississippi 38677*
 (19) *Nagoya University, Chikusa-ku, Nagoya 464 Japan*
 (20) *University of Oregon, Eugene, Oregon 97403*
 (21) *INFN Sezione di Padova and Università di Padova, I-35100 Padova, Italy*
 (22) *INFN Sezione di Perugia and Università di Perugia, I-06100 Perugia, Italy*
 (23) *INFN Sezione di Pisa and Università di Pisa, I-56100 Pisa, Italy*
 (25) *Rutgers University, Piscataway, New Jersey 08855*
 (24) *Rutherford Appleton Laboratory, Chilton, Didcot, Oxon OX11 0QX United Kingdom*
 (26) *Sogang University, Seoul, Korea*
 (27) *Stanford Linear Accelerator Center, Stanford University, Stanford, California 94309*
 (28) *University of Tennessee, Knoxville, Tennessee 37996*
 (29) *Tohoku University, Sendai 980 Japan*
 (30) *Vanderbilt University, Nashville, Tennessee 37235*
 (31) *University of Washington, Seattle, Washington 98195*
 (32) *University of Wisconsin, Madison, Wisconsin 53706*
 (33) *Yale University, New Haven, Connecticut 06511*
- † *Deceased*
 (a) *Also at the Università di Genova*
 (b) *Also at the Università di Perugia*

References

- [1] A. Blondel, B. W. Lynn, F. M. Renard, and C. Verzegnassi, *Nucl. Phys.* **B304**, 438 (1988).
 [2] R. D. Field and R. P. Feynman, *Nucl. Phys.* **B136**, 1 (1978).

- [3] R. Brandelik *et. al.* (TASSO Collaboration), Phys. Lett. **B100** 357 (1981); C. Berger *et. al.* (PLUTO Collaboration), Nucl. Phys. **B214** 189 (1983); W. W. Ash *et. al.* (MAC Collaboration), Phys. Rev. Lett. **58** 1080 (1987); T. Greenshaw *et. al.* (JADE Collaboration), Z. Phys. **C42** 1 (1989); and D. Stuart *et. al.* (AMY Collaboration), Phys. Rev. Lett. **64** 983 (1990).
- [4] D. Buskulic *et. al.* (ALEPH Collaboration), Phys. Lett. **B335** 99 (1994).
- [5] R. Akers *et. al.* (OPAL Collaboration), CERN-PPE/95/50 (1995).
- [6] P. Abreu *et. al.* (DELPHI Collaboration), Z. Phys. **C65**, 569 (1995).
- [7] K. Abe *et. al.*, Phys. Rev. Lett. **74**, 2890 (1995).
- [8] K. Abe *et. al.*, Phys. Rev. Lett. **74**, 2895 (1995).
- [9] K. Abe *et. al.*, Phys. Rev. Lett. **73**, 25 (1994)
- [10] M. Hildreth *et. al.*, SLAC-PUB-6656, Sept, 1994 (submitted to IEEE Trans. Nucl. Sci.).
- [11] G. Agnew *et. al.*, SLAC-PUB-5906 (1992).
- [12] E. Farhi, Phys. Rev. Lett **39**, 1587 (1977).
- [13] D. Axen *et. al.*, Nucl. Inst. and Meth. *A238*, 472 (1993).
- [14] K. Abe *et. al.*, SLAC-PUB-6569, July, 1994 (submitted to Phys. Rev. D).
- [15] Jets are defined with the JADE algorithm, W. Bartel *et. al.*, Z. Phys. **C33**, 23 (1986), using a value of $y_{min} = 0.02$.
- [16] G. Altarelli and B. Lampe, Nucl. Phys. **B391**, 3 (1993).
- [17] B. Lampe, MPI-PH-93-74 (1993).
- [18] T. Sjöstrand, Computer Phys. Commun. **39** 347, (1986); T. Sjöstrand and M. Bengtsson, Comput. Phys. Commun. **43** 367 (1987).
- [19] J. B. Stav and H. A. Olsen, Trondheim U. Preprint 1994-17, (1994).